Hindawi
Journal of Nanotechnology
Volume 2018, Article ID 1236878, 8 pages
https://doi.org/10.1155/2018/1236878

Research Article

Dye-Sensitized Solar Cells Prepared with Mexican Pre-Hispanic Dyes

Mario Alberto Sánchez-García,[1] Xim Bokhimi,[1] Sergio Velázquez Martínez,[2] and Antonio Esteban Jiménez-González[3]

[1]*Institute of Physics, National Autonomous University of Mexico (IF-UNAM), Apartado Postal 20-364, 04510 Mexico City, Mexico*
[2]*Centro de Investigación en Ingeniería y Ciencias Aplicadas de la Universidad Autónoma del Estado de Morelos, Av. Universidad 1001, Col. Chamilpa, 62209 Cuernavaca, Mor, Mexico*
[3]*Institute of Renewable Energy, National Autonomous University of Mexico (IER-UNAM), 62580 Temixco, Mor, Mexico*

Correspondence should be addressed to Antonio Esteban Jiménez-González; ajg@ier.unam.mx

Received 6 December 2017; Revised 6 March 2018; Accepted 31 March 2018; Published 19 June 2018

Academic Editor: Raul Arenal

A dye-sensitized solar cell (DSSC) is a photovoltaic device capable of generating electrical power from the absorption of solar radiation. These cells use a $SnO_2:F/TiO_2$/dye heterojunction as the active electrode (working electrode). Active electrodes containing TiO_2 in the anatase crystalline phase and synthetic dyes are used to achieve high conversion efficiencies. Synthetic dyes, whether organic or organometallic compounds, have the disadvantage of being expensive. For this reason, many efforts are made worldwide to find natural dyes with lower production costs that can be used in the fabrication of DSSCs. *Nocheztli* is a natural red dye obtained from the cochineal insect *Dactylopius coccus*; the dye dates from pre-Hispanic times and contains high levels of carminic acid (CA). *Nocheztli* has been used in Mexico in textile dyeing from pre-Hispanic times to the present. Carmine is an organometallic dye with two molecules of carminic acid and one atom of aluminum in its structure; it is obtained by the interaction of the carminic acid from *Nocheztli* with aluminum salts. Carminic acid and carmine molecules contain a carboxyl group in their structure, allowing them to anchor to TiO_2, creating a suitable heterojunction to prepare DSSCs. In this study, both dyes are used to sensitize the mesoporous $TiO_2{}^m$ semiconductor to prepare DSSCs.

1. Introduction

Since the discovery of TiO_2 dye-sensitized solar cells (DSSCs) by Grätzel and O'Regan in 1991 [1], dyes have become important in the research of new materials to develop solar cells. Such dyes must have certain properties to be used in the design of sensitized solar cells. First, the dye must have anchor groups, such as a carboxyl group, to attach to the surface of an oxide semiconductor such as anatase TiO_2, and it must be able to absorb electromagnetic radiation in the visible region. Second, the dye's lowest unoccupied molecular orbital (LUMO) level—or lowest excited state energy level—must match the lowest TiO_2 conduction band level to achieve an efficient injection of electrons. Third, the energy level in the highest occupied molecular orbital (HOMO) level—or oxidized state of the dye—must be lower than the redox level of the electrolyte used for efficient dye regeneration. Fourth, the dye must be stable enough to withstand 10^8 cycles of excitation/injection/regeneration, equivalent to 20 years of exposure to natural light [2–4]. The characteristics listed above correspond to an ideal photosensitizer or dye for use in DSSCs.

Figure 1 shows the structure of a sensitized solar cell. In the left-hand side of Figure 1, the transparent conductive oxide (TCO), a SnO_2:F layer, is seen deposited on a commercial glass substrate. On the TCO, a (compact) blocking titanium oxide ($TiO_2{}^b$) layer is deposited; on the latter, a mesoporous titanium oxide ($TiO_2{}^m$) layer is grown as an n-type semiconductor material. The $TiO_2{}^m$ layer is later sensitized with the dye. The SnO_2:F/$TiO_2{}^b$/$TiO_2{}^m$/dye arrangement constitutes the working or active electrode of a DSSC. In the right-hand side of

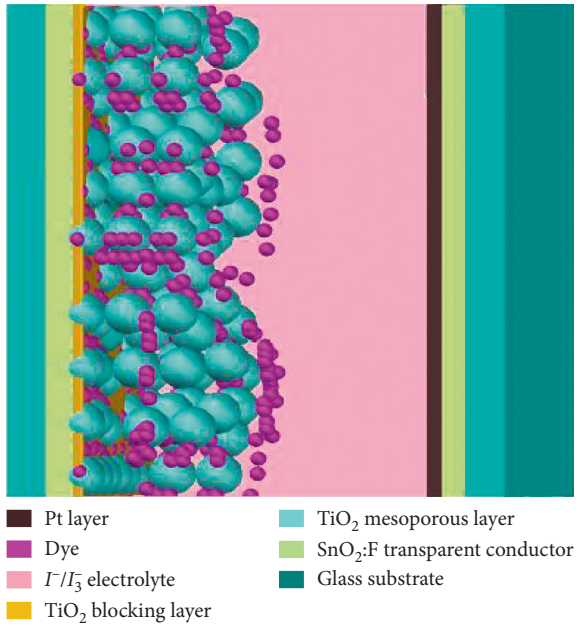

FIGURE 1: Structure of a dye-sensitized mesoporous TiO_2 solar cell.

Figure 1, a TCO (SnO_2:F) layer coated with a thin film of platinum is seen, which constitutes the counterelectrode, whose function is to regenerate the electrolyte. The space between the active electrode and counterelectrode is filled with the electrolyte containing the I^-/I_3^- redox pair.

When illuminating the DSSC, the dye molecules absorb electromagnetic radiation, and for each absorbed photon, an electronic transition is generated from the base state (S) to an excited state (S^*), which is represented by (1) and (2); that is, the electron passes from the HOMO level to the LUMO level of the dye. From this state, the electron is injected into the conduction band of the semiconductor oxide, generating a dye cation (S^+). Therefore, it is necessary to regenerate the dye, and electrons are taken from the iodides (I^-) contained in the electrolytic solution causing them to oxidize and form triiodide ions (I_3^-), which is represented by (3). Finally, triiodide ions are reduced by accepting electrons from the counterelectrode to return to their original state (I^-), which is represented by (4) [2, 3]. The holes formed in the platinum counterelectrode because of donating electrons to the electrolyte recombine with the placed external electric charge to close the electric circuit.

$$S^0 + h\vartheta \longrightarrow S^*, \tag{1}$$

$$S^* \longrightarrow S^+ + e^-_{(\text{injected})}, \tag{2}$$

$$S^+ + \frac{3}{2}I^- \longrightarrow S^0 + \frac{1}{2}I_3^-, \tag{3}$$

$$\frac{1}{2}I_3^- + e^-_{(\text{counterelectrode})} \longrightarrow \frac{3}{2}I^-. \tag{4}$$

One of the most popular dyes used in the manufacturing of DSSCs is N719 (*cis-diisothiocyanato-bis(2,2′-bipyridyl-4,4′-dicarboxylato) ruthenium (II) bis(tetrabutylammonium)*); this is an artificial dye with a central ruthenium atom in its molecular structure and is capable of absorbing photons below 750 nm [5]. The artificial dyes used in the fabrication of DSSCs, such as N719, have allowed for efficiencies higher than 10%. However, the dyes with a ruthenium atom in its molecular structure have a high production cost [4, 6].

Other dyes with a metallic atom in their molecular structure are phthalocyanines and porphyrins, which have also been used to fabricate DSSCs, reaching efficiencies of 3.5% and 7.1%, respectively [7–9].

Because of the high cost of ruthenium dyes, efforts have been made to replace them with organic dyes, which have lower manufacturing and purification costs, although their use is not widespread. With the use of organic dyes in the construction of DSSCs, conversion efficiencies of approximately 9.5% have been reported [10, 11].

Natural dyes are a more economical alternative for DSSC innovation, as they can be extracted from plants, flowers, fruits, and in some cases, minerals and insects [6, 12]. Natural dyes have low production costs and are considered environmentally friendly because of their zero toxicity [13]. The highest efficiencies reported for natural-DSSCs are approximately 2%, as in the case of cells sensitized with the extract of purple plants such as beet (red turnip) and *Dioscorea alata* (purple yam) [4, 14, 15]. Efficiencies of approximately 4% have also been reported for DSSCs using compounds derived from chlorophyll [16, 17].

First, this study reports the preparation and optimization of each DSSC component layer, mainly the TiO_2^b blocking layer, mesoporous TiO_2^m layer, active electrode represented by the SnO_2:F/TiO_2^b/TiO_2^m/dye heterojunctions, and counterelectrode. The optimization of the properties of the component layers is performed through a correlation study between the synthesis parameters of TiO_2^b and TiO_2^m and solar cell performance parameters such as open-circuit voltage (V_{oc}), short-circuit current (J_{SC}), fill factor (FF), and conversion efficiency (η%) of the solar cell.

Second, the study reports the use of dyes derived from the natural dye Nocheztli (carminic acid) and carmine, in the design and innovation of two DSSCs: (a) *SnO_2:F/TiO_2^b/TiO_2^m/carminic acid/redox (I^-/I_3^-)/Pt/SnO_2:F* and (b) *SnO_2:F/TiO_2^b/TiO_2^m/carmine/redox (I^-/I_3^-)/Pt/SnO_2:F*. Additionally, the values obtained from solar cell performance parameters such as V_{oc}, J_{SC}, FF, and η% are presented. This is the first report on the preparation of carmine DSSCs.

2. Materials

2.1. Natural Dye Nocheztli. *Nocheztli* is a natural dye obtained from the hemolymph of the female cochineal insect *Dactylopius coccus*. These insects cluster on nopal cactus pads. The word *"Nocheztli"* comes from the Nahuatl language, spoken by the Aztecs, whose translation means "tuna blood." This dye has been used in Mexico since pre-Hispanic times and has since been highly prized because it was one of the tributes offered to the Aztec Empire [18].

Nocheztli was represented in pre-Columbian writing, used by the Aztecs, as a sack with red dots, as seen in Figure 2(a). Its use and preparation are one of the few skills

(a)

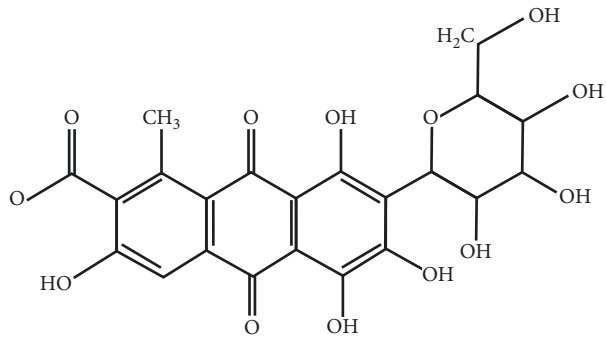

(b)

Figure 2: (a) Representation in codex of the pre-Columbian dye Nocheztli (http://www.wdl.org/es/item/3248/) and (b) molecular structure.

recovered, after the conquest of Mexico by the Spaniards, thanks to the teachers and students surviving the conquest and to the Spanish priests who helped preserve it [19]. The *Nocheztli* dye has been used in Mexico since the time of the Aztec Empire in textile dyeing, among other uses, becoming a high-quality export during the period of occupation of Mexico by the Spaniards. However, it was displaced in the second half of the nineteenth century by synthetic anilines.

Currently, synthetic anilines are widely used as food, drug, and cosmetic dyes, but health problems have arisen. That is why today, carminic acid has again gained interest in these areas because of its lack of toxicity [20, 21].

The body of an adult female cochineal insect contains 10% in weight of carminic acid (CA), which is the main component of *Nocheztli* [22]. CA is *a hydroxyanthraquinone* (*2-α-D-glucopyranosyl-8-methyl-1,3,4,6-tetrahydroxy-anthraquinone-7-carboxylic acid*) [21, 23]. The CA molecule consists primarily of three groups: anthraquinone chromophore, a glucopyranose ring attached by a glycosidic linkage, and a carboxyl group (COOH). The glucopyranose ring is perpendicular to the planar anthraquinone structure (Figure 2(b)) and the carboxyl group. The carboxyl group allows CA to create a chemical bond with a metal cation, for example, Ti (IV), and to "anchor" to a metal oxide, such as TiO_2. Figure 2(b) shows the molecular structure of CA, in which the carboxyl group (COOH) can be seen in the top left-hand side of the structure.

CA changes color depending on the pH of the solvent in which it is immersed [24]. Its tonality varies from yellow-orange (pH = 2) to purple (pH = 13) [25]. The hue change is attributed to the formation of different anions depending on the pH of the solution. For example, at very acidic pH (pH = 2), the CA^{-} anion is formed, whose absorption peak is 490 nm. At neutral pH (pH = 7), the CA^{-2} anion is formed, whose absorption peak is 558 nm. Finally, at very basic pH (pH = 13), the CA^{-3} anion is formed, which has two absorption peaks: 530 nm and 566 nm [26].

2.2. Carmine Dye. Depending on the use of *Nocheztli*, the active dye is either CA or carmine. When an aluminum salt is mixed with the dye, the organometallic compound

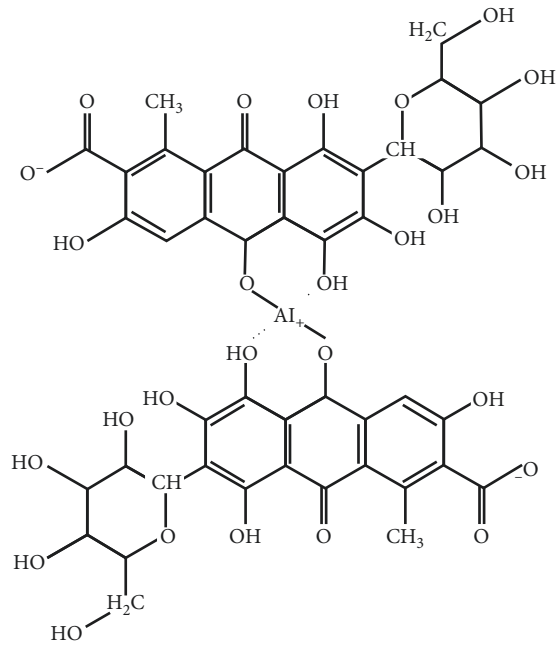

Figure 3: Molecular structure of carmine.

carmine is obtained. For example, in Mexico, in the craft dyeing of textiles, alum ($KAl(SO4)_2{\cdot}12H_2O$) has been added to the solution prepared with *Nocheztli* since pre-Hispanic times.

The carmine molecule is formed by two CA molecules attached to an aluminum atom, as shown in Figure 3 [21]. Carmine has been used by Rosu et al. [27] to demonstrate that TiO_2 can be sensitized by it, making it possible to prepare the TiO_2/carmine heterojunction. Therefore, to date, carmine dye has not been used in the fabrication of DSSCs.

CA and carmine dyes, used for the dye-sensitization experiments with n-type semiconductor TiO_2^m programmed for this study, were purchased from Sigma-Aldrich.

3. Experimental Methods

3.1. Analytical Characterization Techniques. The analytical techniques used to study the structural, optical, and electrical

properties of the TiO_2^b blocking and mesoporous TiO_2^m layers have been already reported elsewhere [28]. The crystalline phase and crystal size of the abovementioned samples was determined on a Rigaku D/MAX 2200 X-ray diffractometer equipped with Cu-Kα radiation ($\lambda = 1.54056$ Å) [29]. Two field-emission scanning electron microscopes (FE-SEMs) were used to study the surface morphology of n-type semiconductors: (a) TiO_2^b blocking layer (JEOL JSM-7800F) and (b) TiO_2^m mesoporous film (Hitachi S-5500). Optical transmittance, specular, and diffuse reflectance spectra of the same samples in thin-film form were recorded on a Shimadzu 2100 ultraviolet-visible (UV-VIS) spectrophotometer. Measurements of I versus V curves used to describe the performance of DSSCs were carried out utilizing equipment already reported [28].

3.2. Preparation of Component Layers and Assembly of DSSCs. The TiO_2^b blocking layer was deposited on a transparent conductive substrate by the sol-gel chemical deposition technique. For the sol-gel technique, a precursor solution of titanium isopropoxide, deionized water, hydrochloric acid, and ethanol was prepared in air at atmospheric pressure following the procedure already reported elsewhere [30]. The transparent conductor was SnO_2:F (TEC15) from Pilkington Group Limited, whose sheet resistance $R_\square$ was 15 Ω.

To deposit a suitable mesoporous layer, TiO_2 nanoparticles were synthesized following the methodology already reported in the literature [28, 31]. First, a mixture of titanium isopropoxide, acetic acid, and nitric acid was prepared and stirred at a continuous stirring speed of 700 rpm. Finally, 150 ml of the mixture was charged in an autoclave with a capacity of 300 ml and then subjected to hydrothermal treatment at 200°C for 12 h. The resulting nanoparticles were rinsed and centrifuged with ethanol and acetone to remove acid residues.

With the TiO_2 nanoparticles, terpineol as a dispersing agent and ethylcellulose used to provide a high porosity, a viscous paste was prepared to carry out the deposition of mesoporous layers of TiO_2^m by the screen-printing technique over a wide range of thicknesses (1 to 100 μm) [28, 32, 33].

To prepare the SnO_2:F/TiO_2^b/TiO_2^m heterojunction as the active electrode of the single DSSC, the following procedure already described in [28] was performed: (a) by using the sol-gel technique, the TiO_2^b compact layer was deposited on the transparent conductor (SnO_2:F) and (b) on the SnO_2:F/TiO_2^b junction, screen-printing of the mesoporous TiO_2^m layer was carried out using the paste described in the last paragraph. A manually operated screen-printing equipment consisting of a 140T mesh and a storage capacity area of $1 \times 0.5\,cm^2$ delimited by a stencil was used to deposit mesoporous layers of TiO_2^m over the SnO_2:F/TiO_2^b junction.

After the deposition of each layer by screen-printing, the mesoporous TiO_2^m layer was heated at 130°C for 3 min. Once all the screen prints were finished, the temperature was increased in intervals of 100°C with a rest time of 10 min between each increment. When the temperature reached 530°C, the mesoporous film was kept at this temperature for 1 h. Table 1 shows thicknesses of mesoporous TiO_2^m layers achieved during this study.

Table 1: Relation between the thicknesses of the used porous TiO_2^m layers and the number of screen-printing depositions.

Number of screen-printing depositions	Thickness d (μm)
1	0.6 ± 0.2
8	4.7 ± 0.9
18	12 ± 3

To fabricate DSSCs, the mesoporous TiO_2^m films with average thicknesses of 4.7 and 12 μm (8 and 18 screen-printing layers) were first deposited on the SnO_2:F/TiO_2^b junction to obtain the SnO_2:F/TiO_2^b/TiO_2^m heterojunctions. CA sensitization of the mesoporous layers in the SnO_2:F/TiO_2^b/TiO_2^m heterojunction was performed as follows: after the heat treatment at 530°C, the heterojunction was allowed to cool to 80°C, and then the heterojunction was immersed in a 0.5 mM solution of CA in anhydrous ethanol for 20 h. However, because carmine is not soluble in ethanol, methanol was used to prepare a 0.5 mM solution with this dye following a procedure similar to that reported in the literature [27]. Later, the obtained active electrodes were washed with the solvent employed (ethanol or methanol) and dried with nitrogen gas before assembling the DSSC.

The preparation of the electrolyte solution was based on those reported in [28, 34–37]. The I^-/I_3^- redox couple was prepared using 0.6 M 1-propyl-3-methyl-imidazolium iodide (PMII; Sigma-Aldrich), 0.1 M lithium iodide (LiI; Sigma-Aldrich), 0.1 M guanidine thiocyanate (GuSCN; Merck), 0.5 M 4-tertbutyl-pyridine (TBP; Sigma-Aldrich), and 0.05 M iodine (I_2; Sigma-Aldrich) in a mixture of 85% acetonitrile (Sigma-Aldrich) and 15% valeronitrile (Sigma-Aldrich; 85%).

The platinum catalyst, obtained from a 40 mM chloroplatinic acid solution (Sigma-Aldrich) in 2-propanol (Sigma-Aldrich), was deposited on the transparent conductor to obtain the SnO_2:F/Pt junction, which was heated at 130°C in air for 3 min to evaporate the solvent. In total, three layers of solution were deposited by the sol-gel technique. Finally, the counterelectrode was subjected to a heat treatment at 400°C in air for 10 min [30].

The solar cell assembly consists of joining the active electrode SnO_2:F/TiO_2^b/TiO_2^m and the counterelectrode SnO_2:F/Pt by means of a spacer Meltonix (Surlyn® polymer), which melts at 230°C. Once the DSSC was sealed, the electrolyte was introduced through a hole drilled in the counterelectrode beforehand, which was later sealed [31]. To improve the electrical conductivity of the electrical contacts to the DSSCs, a layer of silver-conductive paint was applied to the area where they were placed.

4. Results and Discussion

4.1. Analysis of the TiO_2^b Blocking Layer. Figure 4 shows the X-ray diffraction (XRD) pattern of the TiO_2^b blocking layer deposited on Corning glass by the sol-gel chemical deposition technique with a film thickness of $t = 100$ nm. This figure shows that the TiO_2^b blocking layer consists of the anatase crystalline phase (PDF 21-1272) with a dominant reflection along the (101) plane and an average crystal size of

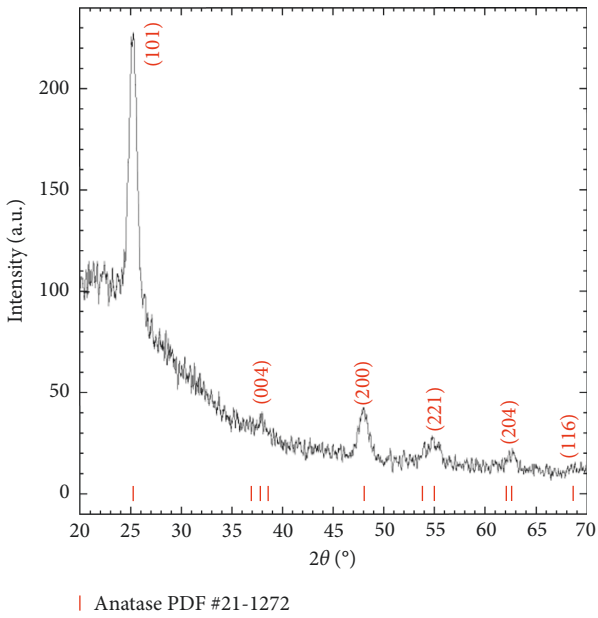

Figure 4: XRD pattern of the TiO_2 blocking layer.

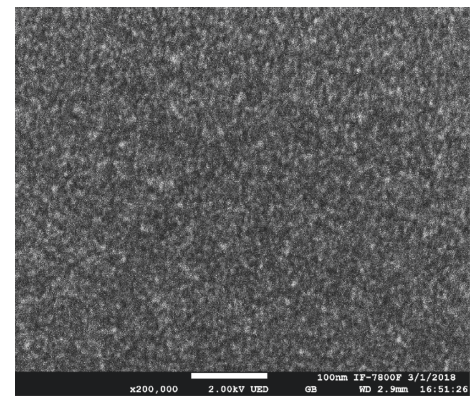

Figure 5: FE-SEM image of the $TiO_2{}^b$ blocking layer.

12 nm. In addition, Figure 5 shows a micrograph of this layer obtained by FE-SEM, in which a compact structure of the anatase crystallites is observed. The compact structure of $TiO_2{}^b$ is essential for blocking the undesirable effects of recombination caused by direct contact between the electrolyte and SnO_2:F. This is why it is called a compact blocking layer. At the same time, the compact layer passivates the mesoporous $TiO_2{}^m$ layer and reduces contact resistance between the mesoporous layer and the conductive glass.

4.2. Characterization of the Mesoporous $TiO_2{}^m$ Layer. The mesoporous $TiO_2{}^m$ layer prepared first through a hydrothermal process at 200°C and under pressure (autoclaving at 54 atm) for 12 h and later heated in air at a temperature of 530°C was analyzed by the X-ray diffraction technique. This layer possess an anatase crystalline phase (PDF 21-1272) whose diffraction pattern coincides with the already shown in Figure 4 for the $TiO_2{}^b$ blocking layer and with a dominant reflection along the (101) plane. The crystal size obtained from the Scherrer equation is 12.4 nm. Acquired by FE-SEM, Figure 6(a) shows a cross-sectional image of the $TiO_2{}^m$ layer where a very homogeneous structure can be observed throughout the layer thickness. Figure 6(b) shows a micrograph of the $TiO_2{}^m$ surface with a homogeneous and mesoporous structure. The QUARTZ PCI software allows one to determine the pore size distribution of these films, and we obtain values of approximately 23.116 ± 4.236 nm. According to IUPAC standards [38], a film is considered mesoporous when it has pore sizes in the range of 2 to 50 nm.

The absorption coefficient (α) for a semiconductor film material is described by the mathematical expression $\alpha = 1/t \ln(100 - R_{sp} - R_{dif}/T\%)$, which is obtained from the optical transmittance (T%), the specular reflectance (R_{sp}), and diffuse reflectance (R_{dif}) of a semiconductor with a film thickness of t. Considering that TiO_2 in the anatase phase has an indirect forbidden band, a curve of $(\alpha h\nu)^{0.5}$ versus $h\nu$ was plotted, from which the indirect forbidden band value $E_g{}^{ind} = 3.34$ eV is obtained for the mesoporous $TiO_2{}^m$ layer. For an average crystal size of 12 nm, the value of $E_g{}^{ind}$ is congruent with anatase TiO_2, which has a reported value in the literature of 3.2 eV [39].

4.3. Optical Absorbance Studies of CA and Carmine. Figure 7 shows the optical absorbance curves of CA and carmine. CA and carmine begin to absorb starting at approximately 610 nm. CA has the highest absorbance intensity (0.56 a.u.) and a total absorbance peak at 497 nm; carmine has a total absorbance peak at 517 and a lower absorbance intensity (0.12 a.u.). If the absorbance curve is integrated, an approximate ratio of dye intensity is found in the following order: carmine (21.44%) < CA (100%). This ratio of absorbance intensities of the electromagnetic radiation must affect the performance of DSSCs.

4.4. CA and Carmine DSSCs. To fabricate the DSSCs, mesoporous $TiO_2{}^m$ layers were used with a thickness of 12 ± 3 μm at the active electrode. Solar cells whose active electrode SnO_2:F/$TiO_2{}^b$/$TiO_2{}^m$ were treated at 530°C exceed in efficiency than those constructed with the same active electrode treated at lower temperatures. The active electrode SnO_2:F/$TiO_2{}^b$/$TiO_2{}^m$ treated at 530°C provides a more compact structure between layers and between grain boundaries, offering better trajectories for the electrons injected into the $TiO_2{}^m$ conduction band. Figure 8 shows the I versus V curves of (a) CA and (b) carmine DSSCs. As a general characteristic of both cases, it is observed that the I-V curves have a very acceptable current-rectifying effect, and under light, show the photovoltaic effect, which means the suitable formation of an n-p semiconductor junction between the $TiO_2{}^m$ n-type semiconductor and CA and carmine dyes.

Table 2 lists the performance parameters obtained for the DSSCs according to the dye used for the sensitization. When comparing the results obtained for both DSSCs, it can be observed that their open-circuit (V_{oc}) values are very similar, 0.443 V for CA and 0.457 V for carmine, while the short-circuit current was higher for CA DSSCs ($J_{SC} = 0.79$ mA/cm^2) than for carmine DSSCs ($J_{SC} = 0.18$ mA/cm^2). However, the

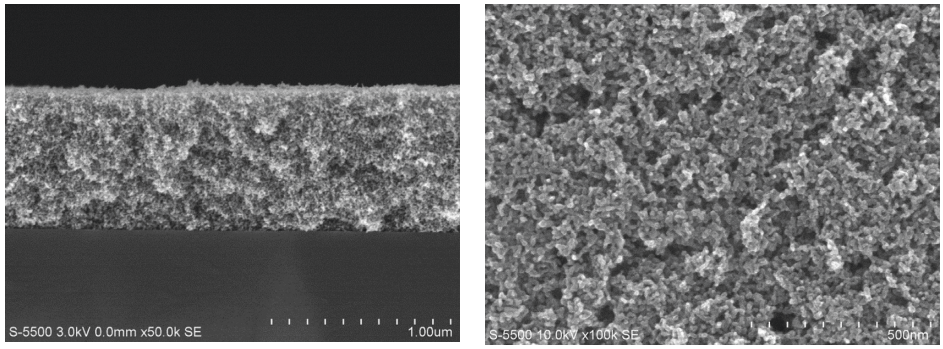

(a) (b)

Figure 6: (a) FE-SEM cross-sectional image of a mesoporous $TiO_2{}^m$ layer. (b) FE-SEM image of the surface of a mesoporous TiO_2 layer.

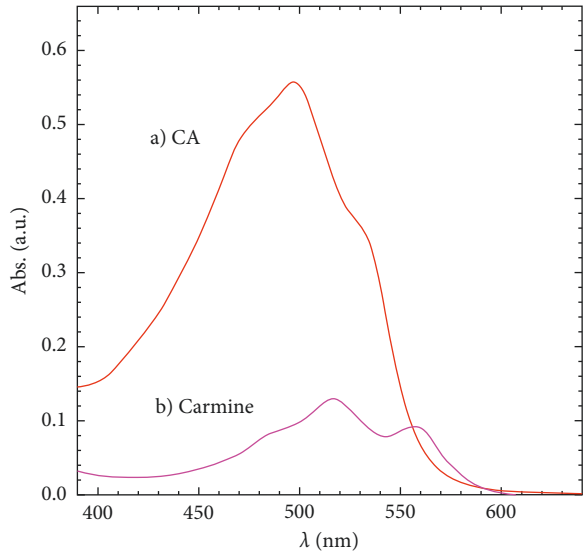

Figure 7: Optical absorbance curves of (a) CA and (b) carmine.

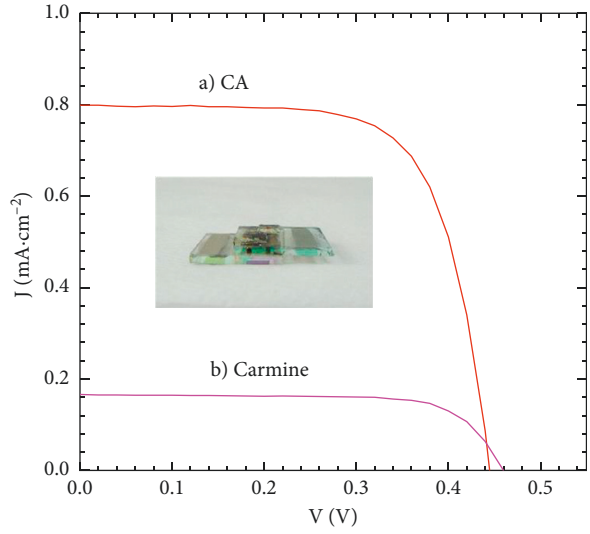

Figure 8: I-V curves of (a) CA and (b) carmine DSSCs.

Table 2: Experimental parameters for CA and carmine DSSCs.

Dye	V_{OC} (V)	J_{SC} (mAcm^{-2})	FF	η%
Carmine	0.457	0.17	0.74	0.06
CA	0.455	0.748	0.71	0.24

values of the fill factor were very similar for both CA DSSCs (FF = 0.71) and carmine DSSCs (FF = 0.74). Fill factor values above 0.7 are very acceptable. Finally, the conversion efficiency of CA DSSCs ($\eta = 0.24\%$) was four times higher than that of carmine DSSCs ($\eta = 0.06\%$).

Considering that the values obtained for V_{oc} and FF are similar for both solar cells, the difference between the values of the conversion efficiency of these solar cells (η%) are determined mainly by the values of J_{SC}. This is likely because CA has a greater capacity to produce photogenerated electrons and, from its excited state, inject these electrons into the $TiO_2{}^m$ conduction band. A possible explanation for why higher short-circuit current values are reached in CA DSSCs than in carmine DSSCs lies in their different capacities to absorb electromagnetic radiation and generate charge carriers. The integrated optical absorbance of CA is six times greater than that of carmine, as seen in Figure 7. In the insert of Figure 8, one of the CA DSSCs is shown.

The absorption intensity of the dye also affects the performance of a DSSC. If the optical properties of the dyes studied here are compared with the ruthenium dye N719 used to fabricate DSSCs whose conversion efficiency is greater than 9%, the intensity of the absorbance spectra of the N719 dye is greater than those of the CA and carmine dyes. N719 has two optical absorption peaks in the visible range of the electromagnetic spectrum, whose values of optical absorbance are 0.58 at 375 nm and 0.63 at 530 nm [40]. It is clear that the absorbance levels of N719 dominate over those corresponding to CA and carmine in an approximate ratio of carmine (14.74%) < CA (68.7%) < N719 (100%). This fact should influence the values of the performance parameters (η%, J_{SC}, V_{oc}, and FF) of each CA and carmine DSSC because the optical absorbance of each material is intimately linked to the generation capacity of charge carriers in the solar cell. In particular, it is considered that the low absorbance levels of

CA and of carmine are responsible for obtaining low short-circuit current (J_{SC}) values.

As explained in Section 2.1, the molecular structure of CA is elongated in the horizontal direction, with a single carboxyl group at the left end of the molecule through which CA binds to TiO_2. The rest of the structure, composed of the R group, includes the anthraquinone chromophore in the middle part and the glucopyranose ring at the right end. With this configuration, the elongated structure of the R group favors steric hindrance so that the pigment forms a weaker bond with the TiO_2 oxide surface and, thus, prevents the molecule from being attached to TiO_2 effectively. This causes a weak transfer of electrons from the dye molecules to the TiO_2 conduction band [4].

Natural dye sensitizers in DSSCs generally give low conversion efficiencies in the order of 1% or less. This is in part due to the existence of OH- and O-ligands, as they appear in the molecular structure of CA and carmine (Figures 2(b) and 3), which hinder the interaction with TiO_2 and prevent efficient electron transfer from the dye molecules to the TiO_2 conduction band. In contrast, most synthetic dyes contain a greater number of COOH groups and almost no OH- or O-ligands. For example, the synthetic dyes N3 and N179 have a more symmetrical structure around the ruthenium atom. The N3 dye has four carboxyl groups in its molecular structure, and N719 has two; this allows them to interact with TiO_2 more efficiently and lead to a greater injection of electrons, generate a higher current density, and thus, exhibit a higher conversion efficiency.

In general, natural dyes suffer from low V_{oc}. This may be because of possible inefficient electron/cation recombination pathways and the acidic dye adsorption environment [14]. In fact, once adsorbed, H^+ ions determine the potential at the surface of TiO_2, and this adsorption of protons causes a positive displacement of the Fermi level of the TiO_2, thus limiting the maximum photovoltage that could be supplied by the solar cells. Looking at the literature, one finds that CA has already been used to sensitize DSSCs, through which efficiencies of 0.1% have been achieved [41, 42]. In this study, we report a higher efficiency for the same CA DSSC, that is, $\eta = 0.24\%$. Although carmine dyes have already been used by Rosu et al. [27] to prepare the TiO_2/carmine heterojunction, the manufacture of a carmine DSSC has never been reported in the literature.

5. Conclusions

The pre-Hispanic dyes *Nocheztli* (CA) and carmine were used to sensitize the n-type mesoporous TiO_2 semiconductor and, thereby, prepare DSSCs. The n-type mesoporous and nanostructured TiO_2 semiconductor was prepared by a hydrothermal process so that a fine white powder with an anatase crystalline structure was obtained. With this powder, it was possible to prepare mesoporous $TiO_2{}^m$ layers by screen-printing. The highest efficiency of these DSSCs was obtained in those solar cells whose mesoporous layer was baked at 530°C. The DSSCs in which CA and carmine were used to sensitize the mesoporous $TiO_2{}^m$ layer generated electrical power that could be evaluated from their I-V curves. The conversion efficiency of CA DSSCs ($\eta = 0.24\%$) was four times higher than that of the carmine DSSCs ($\eta = 0.06\%$). An explanation for the low efficiencies of CA and carmine DSSCs lies in their low optical absorbance levels in the UV-Vis spectrum compared with organometallic dyes that have high conversion efficiencies. On the other hand, the optical absorbance of CA is approximately six times greater than that of carmine; this favors CA DSSCs over carmine DSSCs in achieving better performance and greater conversion efficiencies. The conversion efficiency of CA DSSCs during this study exceeds that reported in the literature, which is 0.1% efficiency [41, 42]. This is the first report of the preparation of carmine DSSCs.

Conflicts of Interest

The authors declare that they have no conflicts of interest.

Acknowledgments

This study was performed with financial support from the Energy Sustainability Fund SENER-CONACYT-Mexico through Project CEMIE-Sol/2074560/P27. The authors thank Eng. Rogelio Morán Elvira for his support in the scanning electron microscopy measurements and Maria Luisa Ramón García, M.Sc., for her support in measuring and analyzing the X-ray diffraction patterns of the TiO_2 blocking and mesoporous layers.

References

[1] B. O'Regan and M. Grätzel, "A low-cost, high-efficiency solar cell based on dye-sensitized colloidal TiO_2 films," *Nature*, vol. 353, pp. 737–740, 1991.

[2] M. Grätzel, "Review: dye-sensitized solar cells," *Journal of Photochemistry and Photobiology C: Photo-chemistry Reviews*, vol. 4, no. 2, pp. 145–153, 2003.

[3] M. Grätzel, "Conversion of sunlight to electric power by nanocrystalline dye-sensitized solar cells," *Journal of Photochemistry and Photobiology A: Chemistry*, vol. 164, no. 1–3, pp. 3–14, 2004.

[4] M. R. Narayan, "Review: dye sensitized solar cells based on natural photosensitizers," *Renewable and Sustainable Energy Reviews*, vol. 16, pp. 208–215, 2012.

[5] M. Grätzel, "Solar energy conversion by dye-sensitized photovoltaic cells," *Inorganic Chemistry*, vol. 44, no. 20, pp. 6841–6851, 2005.

[6] N. A. Ludin, A. M. Al-Alwani Mahmoud, A. B. Mohamad, A. H. Kadhum, K. Sopian, and N. S. Abdul Karim, "Review on the development of natural dye photosensitizer for dye-sensitized solar cells," *Renewable and Sustainable Energy Reviews*, vol. 31, pp. 386–396, 2014.

[7] N. Robertson, "Catching the rainbow: light harvesting in dye-sensitized solar cells," *Angewandte Chemie International Edition*, vol. 47, no. 6, pp. 1012–1014, 2008.

[8] J.-J. Cid, J.-H. Yum, S.-R. Jang et al., "Molecular cosensitization for efficient panchromatic dye-sensitized solar cells," *Angewandte Chemie International Edition*, vol. 46, no. 44, pp. 8358–8362, 2007.

[9] W. M. Campbell, K. W. Jolley, P. Wagner et al., "Highly efficient porphyrin sensitizers for dye-sensitized solar cells," *Journal of Physical Chemistry C*, vol. 111, no. 32, pp. 11760–11762, 2007.

[10] A. Mishra, M. K. R. Fischer, and P. Baeuerle, "Metal-free organic dyes for dye-sensitized solar cells: from structure: property relationships to design rules," *ChemInform*, vol. 40, no. 24, pp. 2474–2499, 2009.

[11] S. Ito, H. Miura, S. Uchida et al., "High-conversion-efficiency organic dye-sensitized solar cells with a novel indoline dye," *Chemical Communications*, no. 41, pp. 5194–5196, 2008.

[12] M. M. Noor, M. H. Buraidah, M. A. Careem, S. R. Majid, and A. K. Arof, "An optimized poly (vinylidene fluoride-hexafluoropropylene)-NaI gel polymer electrolyte and its application in natural dye sensitized solar cells," *Electrochimica Acta*, vol. 121, pp. 159–167, 2014.

[13] S. Ali, T. Hussain, and R. Nawaz, "Optimization of alkaline extraction of natural dye from Henna leaves and its dyeing on cotton by exhaust method," *Journal of Cleaner Production*, vol. 17, no. 1, pp. 61–66, 2008.

[14] G. Calogero, G. Di Marco, S. Cazzanti et al., "Efficient dye-sensitized solar cells using Red Turnip and Purple Wild Sicilian Prickly pear fruits," *International Journal of Molecular Sciences*, vol. 11, no. 1, pp. 254–267, 2010.

[15] K. Wattananate, C. Thanachayanont, and N. Tonanon, "ORAC and VIS spectroscopy as a guideline for unmodified red–purple natural dyes selection in dye-sensitized solar cells," *Solar Energy*, vol. 107, pp. 38–43, 2014.

[16] H. Hug, M. Bader, P. Mair, and T. Glatzel, "Biophotovoltaics: natural pigments in dye-sensitized solar cells," *Applied Energy*, vol. 115, pp. 216–225, 2013.

[17] X.-F. Wang, A. Matsuda, Y. Koyama et al., "Effects of plant carotenoid spacers on the performance of a dye-sensitized solar cell using a chlorophyll derivative: enhancement of photocurrent determined by one electron-oxidation potential of each carotenoid," *Chemical Physics Letters*, vol. 423, no. 4–6, pp. 470–475, 2006.

[18] K. Ross, *Codex Mendoza Aztec Manuscript*, Miller Graphics, Productions Liber S.A., CH-Fibrourgh, Switzerland, 1978.

[19] X. Bokhimi, "Recovery of the knowledge in science and technology of the millennial Mexico," in *The Materials Science and its Impact in the Archaeology*, A. D. Mendoza, A. J. A. Arenas, S. J. L. Ruvalcaba, and L. V. Rodriguez, vol. 3, Innovación Editorial Lagares, Naucalpan de Juárez, Mexico, 2006.

[20] I. A. Ibarra, S. Loera, H. Laguna, E. Lima, and V. Lara, "Irreversible adsorption of an aztec dye on fractal surfaces," *Chemistry of Materials*, vol. 17, no. 23, pp. 5763–5769, 2005.

[21] R. W. Dapson, "The history, chemistry and modes of action of carmine and related dyes," *Biotechnic and Histochemistry*, vol. 82, no. 4-5, pp. 173–187, 2007.

[22] Y. Shirata, *Colorantes Naturales de México*, Sanei Process, Tokyo, Japan, 2007.

[23] Y. Caro, L. Anamale, M. Fouillaud, P. Laurent, T. Petit, and L. Dufosse, "Natural hydroxyanthraquinoid pigments as potent food grade colorants: an overview," *Natural Products and Bioprospecting*, vol. 2, no. 5, pp. 174–193, 2012.

[24] R. Pontón-Zúñiga, *Tintorería Mexicana: Colorantes Naturales*, Gobierno del estado de México, Mexico, 2007.

[25] F. Samari, B. Hemmateenejad, and M. Shamsipur, "Spectrophotometric determination of carminic acid in human plasma and fruit juices by second order calibration of the absorbance spectra–pH data matrices coupled with standard addition method," *Analytica Chimica Acta*, vol. 667, no. 1, pp. 49–56, 2010.

[26] M. V. Cañamares, J. V. Garcia-Ramos, C. Domingo, and S. Sanchez-Cortes, "Surface-enhanced Raman scattering study of the anthraquinone red pigment carminic acid," *Vibrational Spectroscopy*, vol. 40, no. 2, pp. 161–167, 2006.

[27] M.-C. Rosu, R.-C. Suciu, M. Mihet, and I. Bratu, "Physical–chemical characterization of titanium dioxide layers sensitized with the natural dyes carmine and morin," *Materials Science in Semiconductor Processing*, vol. 16, no. 6, pp. 1551–1557, 2013.

[28] M. A. Sánchez-García, X. Bokhimi, A. Maldonado-Álvarez, and A. E. Jiménez-González, "Effect of anatase synthesis on the performance of dye-sensitized solar cells," *Nanoscale Research Letters*, vol. 10, no. 1, pp. 306–318, 2015.

[29] B. E. Warren, *X-Ray Diffraction*, Dover Publications Inc., New York, NY, USA, 1990.

[30] S. Gelover, P. Mondragón, and A. Jiménez, "Titanium dioxide sol–gel deposited over glass and its application as a photocatalyst for water decontamination," *Journal of Photochemistry and Photobiology A: Chemistry*, vol. 165, no. 1–3, pp. 241–246, 2004.

[31] S. Ito, T. N. Murakami, P. Comte et al., "Fabrication of thin film dye sensitized solar cells with solar to electric power conversion efficiency over 10%," *Thin Solid Films*, vol. 516, no. 14, pp. 4613–4619, 2007.

[32] H. Kipphan, *Handbook of Print Media*, Springer–Verlag, Berlin, Germany, 2001.

[33] T. B. McSweeney, *Screen Printing. Coatings Technology Handbook*, Marcel Dekker, New York, NY, USA, 1991.

[34] P. Wang, S. M. Zakeeruddin, P. Comte, R. Charvet, R. Humphry-Baker, and M. Grätzel, "Enhance the performance of dye-sensitized solar cells by co-grafting amphiphilic sensitizer and hexadecylmalonic acid on TiO_2 nanocrystals," *Journal of Physical Chemistry B*, vol. 107, no. 51, pp. 14336–14341, 2003.

[35] Q. Wang, J.-E. Moser, and M. Grätzel, "Electrochemical impedance spectroscopic analysis of dye-sensitized solar cells," *Journal of Physical Chemistry B*, vol. 109, no. 31, pp. 14945–14953, 2005.

[36] N. M. Gómez-Ortíz, I. A. Vázquez-Maldonado, A. R. Pérez-Espadas, G. J. Mena-Rejón, J. A. Azamar-Barrios, and G. Oskam, "Dye-sensitized solar cells with natural dyes extracted from achiote seeds," *Solar Energy Materials and Solar Cells*, vol. 94, no. 1, pp. 40–44, 2009.

[37] X. Fang, T. Ma, G. Guan, M. Akiyama, and E. Abe, "Performances characteristics of dye-sensitized solar cells based on counter electrodes with Pt films of different thickness," *Journal of Photochemistry and Photobiology A: Chemistry*, vol. 164, no. 1–3, pp. 179–182, 2003.

[38] L. B. McCusker, F. Liebau, and G. Engelhardt, "Nomenclature of structural and compositional characteristics of ordered microporous and mesoporous materials with inorganic hosts," *Pure and Applied Chemistry*, vol. 73, no. 2, pp. 381–394, 2001.

[39] S. Banerjee, J. Gopal, P. Muraleedharan, A. K. Tyagi, and Baldev Raj, "Physics and chemistry of the photocatalytic titanium dioxide: visualization of bactericidal activity using atomic force microscopy," *Current Science*, vol. 90, no. 10, pp. 1378–1383, 2006.

[40] K. Hara and H. Arakawa, *Dye–Sensitized Solar Cells. Handbook of Photovoltaic Science and Engineering*, John Wiley & Sons, Hoboken, NJ, USA, 2011.

[41] P. De Padovaa, M. Lucci, B. Olivieri et al., "Natural hybrid organic inorganic photovoltaic devices," *Superlattices and Microstructures*, vol. 45, no. 6, pp. 555–563, 2009.

[42] K.-H. Park, T.-Y. Kim, S. Han et al., "Light harvesting over a wide range of wavelength using natural dyes of gardenia and cochineal for dye-sensitized solar cells," *Spectrochimica Acta Part A: Molecular and Biomolecular Spectroscopy*, vol. 128, pp. 868–873, 2014.